

Clinical usefulness of novel cardiac MDCT/SPECT fusion image

Shinro Matsuo · Kenichi Nakajima · Nasima Akhter · Hiroshi Wakabayashi · Junichi Taki · Koichi Okuda · Seigo Kinuya

Received: 1 April 2009 / Accepted: 26 May 2009 / Published online: 2 July 2009
© The Japanese Society of Nuclear Medicine 2009

Abstract

Background We evaluated the relationship between computed tomography angiography (CTA) and SPECT, and assessed to determine the clinical usefulness of the fusion image using CTA and myocardial perfusion imaging (MPI).

Methods Forty-one consecutive patients [after coronary artery bypass operation ($n = 13$) and suspected stenosis ($n = 28$)] underwent MPI and CTA. SPECT/CTA fused images were generated.

Results In total, 687 segments including bypass graft in 164 coronary arteries were analyzed. Myocardial ischemia on MPI was observed in 11 patients among 28 with CTA abnormalities, one had both ischemia and infarction, and 7 had only infarction. Segment-based analysis showed that ischemia was found in 14 segments (24%) among 59 stenoses on CTA. Forty stenotic segments (69%) were not associated with perfusion abnormality. The rest 5 stenotic segments were considered equivocal (8%). A fusion image made it possible to associate perfusion defects with its corresponding coronary artery in 4 out of 5 equivocal lesions on side-by-side analysis. Patients with incremental diagnostic information on SPECT/CTA fusion ($n = 4$) had significant smaller coronary diameter than that of not-improved coronary vessels (2.0 ± 0.4 vs. 3.9 ± 0.4 mm, $p = 0.001$).

Conclusion Cardiac fusion imaging accurately diagnosed functionally relevant coronary stenosis. SPECT/CTA fusion images in coronary artery disease may provide

added diagnostic information on functional relevance of coronary artery disease.

Keywords Fusion image · CT angiography · Culprit lesion · SPECT

Introduction

Coronary artery disease (CAD) is the leading cause of death in Japan. Nuclear cardiologic studies contribute greatly to guiding management decisions for identifying patients with suspected or known CAD who require catheterization with consideration of coronary intervention [1–3]. Regional myocardial perfusion is often evaluated by stress myocardial single-photon emission computed tomography (SPECT). Recent advances in computed tomography angiography (CTA) have made it possible to identify atherosclerotic lesions in coronary vessels [4, 5]. A physician then views SPECT images and integrates mentally myocardial perfusion imaging (MPI) and anatomical imaging such as CTA or coronary angiography [6, 7]. Therefore, image registration between MPI and anatomical images should improve the diagnosis of culprit coronary lesions that cause myocardial ischemia and provide useful information for decision-making of coronary intervention [8]. Recently, software-based 3D cardiac SPECT/CTA fusion imaging could be clinically used between CTA and SPECT in a company [9–12]. Although creation of a fusion image has various kinds of procedures, there is a report about diagnosis by a single maker using commercial software [6]. However, a creation of the SPECT/CTA fusion imaging in different manufacturers is not yet established.

The aims of this study were to evaluate the relationship of the results between CTA and SPECT, and to determine

S. Matsuo (✉) · K. Nakajima · N. Akhter · H. Wakabayashi · J. Taki · K. Okuda · S. Kinuya
Department of Nuclear Medicine, Kanazawa University Hospital, 13-1 Takara-machi, Kanazawa 920-8641, Japan
e-mail: smatsuo@nmd.m.kanazawa-u.ac.jp

the clinical usefulness of the fusion image using 64-slice CTA and perfusion imaging.

Materials and methods

Patients

Forty-one consecutive patients (13 cases after coronary artery bypass operation and 28 cases with suspected stenosis) underwent CTA and myocardial SPECT. Patients' characteristics are summarized in Table 1. Figure 1 shows a schematic outline of image registration procedure to make cardiac fusion images. The interval of the two examinations of CTA and myocardial SPECT was 19 ± 13 days. There was no cardiac event between the two examinations in each subject.

Table 1 Clinical characteristics of the study group ($n = 41$)

Characteristics	
Age (years)	64 ± 16
Females/males	18/23
Height (cm)	160 ± 10
Weight (kg)	59 ± 12
Cardiovascular risk factors	N (%)
Diabetes mellitus	20 (49)
Hypertension	24 (59)
Dyslipidemia	16 (39)
Medical history	
Previous PCI	4 (10)
Previous CABG	13 (32)

PCI percutaneous coronary intervention, CABG coronary artery bypass grafting

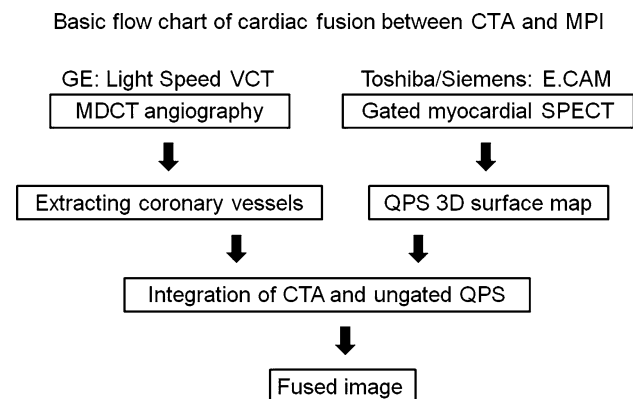


Fig. 1 A schematic outline of image registration procedure to make cardiac fusion images

Computed tomography angiography

CT was performed on a 64-detector CT scanner (Light Speed VCT; GE Healthcare). Scan parameters for CTA were detector collimation, 64×0.625 mm; total z-axis detector coverage, 40 mm; gantry rotation time, 0.35 s; tube voltage, 120 kV; ECG-modulated tube current, 28–750 mA; and pitch, 0.16–0.24, depending on patient's heart rate. A bolus of contrast agent (Iomeron350, Eisai Co., Ltd, Japan) was continuously injected into antecubital vein. ECG-gated image reconstruction methods have been described previously [5, 13]. Sublingual nitroglycerin (0.3 mg) was administered 5 min prior to the scan. After imaging at the level of the carina and positioning the region of interest in the ascending aorta, a bolus of 20 ml of the contrast agent was injected intravenously at 3.3 ml/s via antecubital vein, and the time interval between contrast agent injection and the maximum enhancement within the region of interest was measured. The remainder of the contrast medium (80 ml) was injected and the scan was started according to the transit time that was determined previously.

We investigated the proximal and middle segments of the coronary artery tree, which include the proximal, middle, distal segments and posterior lateral branch of the right coronary artery (RCA), the left main artery, the proximal and middle and distal segments of the left anterior descending (LAD) coronary artery, and the proximal and middle segments of the left circumflex (LCX) coronary artery, according to AHA guidelines [14]. The degree of coronary stenosis and the presence of total occlusion were assessed by visual inspection of curved multiplanar reconstruction (MPR) images and cross-sectional images or oblique MPR images. The assessment was applied to the four major coronary arteries. The four major coronary epicardial arteries were assessed as having hemodynamically significant coronary artery stenosis ($\geq 50\%$ in diameter) or not [5].

Stress MPI

All patients underwent stress ^{99m}Tc -sestamibi (MIBI) or ^{99m}Tc -tetrofosmin imaging. In 15 patients, MPI was performed at the time of exercise with 1-day stress–rest sequence protocol as symptom-limited multi-step exercise using a bicycle ergometer [15]. ^{99m}Tc -MIBI or ^{99m}Tc -tetrofosmin (300–370 MBq) was administered when submaximal heart rate, chest pain, ST-segment depression, or leg fatigue occurred. A standard 12-lead ECG was monitored continuously during the stress procedure and it was printed every minute. An ischemic response was defined as ≥ 1 -mm flat or down-sloping, ST-segment depression or ≥ 1.5 -mm up-sloping, ST-segment depression in ≥ 2

contiguous lead at 80 ms from the J point. Then, exercise was continued for 1 min at the same level as before. Pharmacological stress by adenosine was performed in the remaining 26 patients. Adenosine was administered intravenously at a standard infusion rate of 120 $\mu\text{g}/\text{kg}/\text{min}$ for 6 min. No exercise was done during the infusion. The tracer ($^{99\text{m}}\text{Tc}$ -MIBI or $^{99\text{m}}\text{Tc}$ -tetrofosmin) was injected at 3 min into the adenosine infusion. After the stress image acquisition, the patients were given the tracer (740 MBq) while at rest. After 30 min, ECG-gated image acquisition was started. Patients were asked to discontinue β -blockers and caffeine for 24 h prior to the study. In both protocols, ECG-gated SPECT images were acquired with a 64×64 matrix, 6° step and 360° rotation using a dual-head detector camera (Symbia T6, Siemens Co. Tokyo, Japan) with low-energy high resolution collimator without X-ray-based attenuation correction. The division of the R–R interval was 16.

Image interpretation

Single-photon emission computed tomography images were scored semi-quantitatively by two experienced nuclear cardiologists (S.M., K.N.) using a 17-segment model of the left ventricle with a 5-point scale (0 normal uptake, 1 mild hypoperfusion, 2 moderate hypoperfusion, 3 severe hypoperfusion and 4 no uptake). Summed stress score (SSS) and summed rest score (SRS) were calculated by adding the scores of 17 segments on the stress and the rest images, respectively [16]. Summed difference score (SDS) was derived as the difference between the stress and rest scores. Interpretations were classified into 4 categories: (1) normal (homogenous uptake), (2) ischemia (perfusion defects on post-stress images that completely or partially corrected on rest images, $\text{SDS} \geq 1$), (3) infarct (fixed defect was defined as a region with a score at stress >1 without an improvement at rest), and (4) equivocal. Interpretation classified as equivocal included studies with mild to moderate decreased uptake that could not definitely be classified as normal, ischemia, or infarct [17]. Interpretation could not be confirmed as hypoperfused segment because it was suspected of inferior attenuation or just small size of perfusion defect [17]. The ECG-gated SPECT was quantitatively analyzed with gated QGS/QPS software (Cedars QGS/QPS; Cedars-Sinai Medical Center, Los Angeles, CA) [11].

Fusion of SPECT/CTA

All data were transferred to Siemens hardware for registration and conversion using software of QPS 2008 version [Cedars-Sinai's software (CT fusion)] [11]. An image registration of SPECT and CTA was performed by pixel-shift manual registration using the left ventricular myocardium

as an internal marker. The contour of the heart from the SPECT manually aligned in the position of the vessel from CTA. This positioning also did not change until a later interpretation of fusion imaging in principle. The CT fusion software is capable of combining extracted vascular trees with QPS quantitative 3D surface perfusion maps [5].

Side-by-side interpretation: SPECT plus CTA

Two experienced nuclear cardiologists analyzed the non-fused SPECT–MPI and CTA images side-by-side with regard to functionally relevant coronary stenoses, and consensus was found in every patients. A lesion in any native or bypass graft vessel associated with matching perfusion defects in its corresponding myocardial territory was considered functionally relevant. Furthermore, the CTA findings were compared with the results from invasive coronary angiography to ascertain CTA diagnostic accuracy. All the unevaluable segments were censored as positive and were included in the analysis.

Fused interpretation: SPECT/CTA

The fused 3D SPECT/CTA image analysis was compared with the side-by-side analysis with regard to the interpretation of coronary lesion. First, the readers evaluated whether the fused image provided any additional diagnostic information about the anatomic relationship between perfusion defects and coronary vessels. Additional diagnostic information was considered to be present if the fused images (a) modified the initial interpretation with regard to the relationship between the “culprit lesion” and the corresponding defect or (b) increased the diagnostic confidence for intermediate lesions or equivocal defects. Furthermore, a potential clinical utility was evaluated by retrospectively assessing whether the information increment provided by the fused image would have any impact on the patient's management [6].

Invasive coronary angiography

Invasive coronary angiography was performed using the trans-femoral Judkins approach in three projections in patients who were suspected of CAD on MPI. All angiograms were recorded digitally and quantitatively interpreted off-line by experienced readers. The stenoses were located using the AHA guidelines [15]. Angiographic results were used for comparison with CTA findings. The coronary arteries were quantitatively assessed with the use of an automated edge-detection system (CardioAgent ver. 2.05, Toshiba Medical Systems Co., Tokyo, Japan). Quantitative coronary angiographic measurements were performed for culprit lesion in two image planes and the diameters of the

reference vessel were obtained at the proximal and distal ends of the stenosis. For biplane assessment, diameters obtained in both image planes were averaged. Coronary diameters using invasive coronary angiogram were compared between the vessels with improved interpretation by fusion image and those without improvement.

Statistical analysis

Statistical analysis was performed using a computer-based program. Statistical Discovery Software JMP (version 5.0.1, SAS institute, Cary, NC). A two-tailed Student's *t* test was used for comparison of means. The improved interpretation by fusion image was compared by applying the χ^2 test. All numeric variables are given as mean \pm SD. Categorical data are given in percentages. A two-tailed Student's *t* test was used for comparison of means.

Results

64-slice MDCT finding

Forty-one subjects were in sinus rhythm. Distribution (%) of diagnostic findings on stress SPECT and CTA in 41 patients with or suspected CAD is shown in Table 2. Twenty-eight patients (68%) had significant obstructive coronary arteries ($\geq 50\%$), 4 patients had less than 50% stenosis (10%), and 9 patients had normal coronary artery (22%). Segment-based analysis revealed that, in total, 687 coronary segments including bypass graft in 164 coronary arteries. A stenosis $\geq 50\%$ was found in 64 evaluable segments (9.3%). Four segments (0.5%) were heavily calcified, and 3 segments had intracoronary stents that rendered a reliable analysis, and one segment with motion artifacts was censored as impossible to analyze. Three cases had coronary arteriovenous fistula, two had a coronary vessel from proximal LAD to pulmonary artery, and one had a vessel from RCA to pulmonary artery.

Myocardial perfusion imaging

Myocardial perfusion images could be analyzed for 41 of 41 patients. Visual image analysis revealed that 19 patients (48%) had regional perfusion abnormalities. Twelve of these perfusion abnormalities included ischemic change (fill-in of the tracer). In stress images, mildly abnormal perfusion were found in 9 patients; 2 patients had moderately abnormal perfusion. One had severely abnormal perfusion defect. Of 12 reversible perfusion defects, 6 were in the LAD coronary artery and 4 in the LCX coronary artery and 2 in the RCA. Twenty-two patients showed no perfusion abnormalities on SPECT images. The relation between score of SPECT and

Table 2 Distribution (%) of diagnostic findings on stress single-photon emission computed tomography (SPECT) and computed tomography angiography (CTA) in 41 patients with or suspected coronary artery disease

SPCET findings	Number (%)
Normal	22 (54)
Ischemia	11 (27)
Infarction	7 (17)
Ischemia + infarction	1 (2)
CTA findings	
Normal	9 (22)
<50% Stenosis	4 (10)
$\geq 50\%$ Stenosis	28 (68)

Table 3 The relation between score of SPECT and CTA

	SSS	SRS	Abnormal CTA (%)
Ischemia (<i>n</i> = 11)	3.7 \pm 1.8	0.6 \pm 1.2	9 (82%)
Infarction (<i>n</i> = 7)	5.1 \pm 5.2	4.0 \pm 2.8	5 (71%)
Ischemia + infarction	5	3	1 (100%)
Normal test (<i>n</i> = 22)	0.36 \pm 0.7	0.14 \pm 0.5	13 (59%)

SSS summed stress score, SRS summed rest score

CTA is shown in Table 3. All summed perfusion scores were significantly higher in patients with abnormal SPECT than that in patients with normal SPECT [SSS, 4.2 \pm 3.5 vs. 0.36 \pm 0.7 ($p < 0.0001$); SRS, 1.8 \pm 2.6 vs. 0.14 \pm 0.48 ($p = 0.006$); SDS, 2.3 \pm 2.0 vs. 0.22 \pm 0.53 ($p < 0.0001$)]. The SSS and SRS were significantly higher in patients with fixed perfusion abnormalities than that in those without fixed perfusion abnormalities [SSS, 5.1 \pm 5.3 vs. 1.5 \pm 2.0 ($p = 0.003$); SRS, 3.9 \pm 2.9 vs. 0.3 \pm 0.9 ($p = 0.0001$)]. SDS was higher in patients with fill-in of the tracer (ischemia) compared to those without ischemia [SDS, 3.0 \pm 1.6 vs. 0.4 \pm 0.4 ($p < 0.0001$)]. Ischemic ECG changes during stress occurred in 4 patients. Three of them had small perfusion abnormalities, and one had normal perfusion.

Findings of side-by-side analysis of SPECT and CTA

Figure 2 shows the interrelationship of clinically significant, abnormal diagnostic test results. Myocardial ischemia on SPECT images were observed in 11 cases among 28 with CTA abnormalities, one had both ischemia and infarction, and 7 cases were demonstrated to have only infarction. Sixteen patients had both abnormal diagnostic tests, whereas 3 patients had abnormal perfusion without significant stenosis. Sixteen patients had significant stenosis ($\geq 50\%$) without perfusion abnormalities.

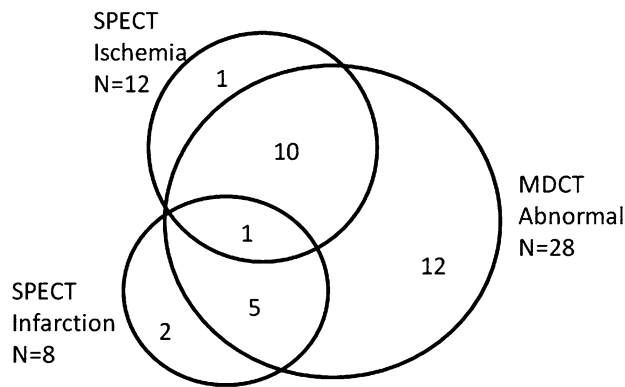


Fig. 2 Venn diagram showing the interrelationship between abnormal MDCT and perfusion abnormalities on SPECT, including ischemia and infarction

Myocardial ischemia was found in 14 segments among 59 stenoses on CTA. Forty segments (69%) with stenosis were not associated with perfusion abnormality; therefore, were classified as hemodynamically irrelevant. Five segments with stenosis were considered equivocal (8%). In one case, there was an ischemia without stenosis on CTA.

Finding of myocardial SPECT/CTA fusion and invasive coronary angiography

A myocardial SPECT/CTA fusion could be created in all 41 subjects. Of the 5 equivocal coronary lesions on side-by-side analysis, 4 were associated with perfusion defects in its corresponding coronary artery territory and, therefore, were considered hemodynamically relevant.

In 18 of the 41 patients (44%), an invasive coronary angiography was performed. Three of 18 patients had intact coronary angiogram and fifteen patients had abnormal coronary vessels. Ten of the 15 patients had stenotic region and considered as culprit lesion on CTA and five patients had equivocal lesion on CTA. Four of the five equivocal coronary lesions could be allocated appropriate coronary stenosis in invasive coronary angiography based on SPECT/CTA fusion image. One of the five equivocal lesions could not be determined as culprit lesion. If we compare the vessel with improved diagnosis by fusion and the vessel of already determined as culprit lesion on CTA, patients with incremental diagnostic information on SPECT/CTA fusion ($n = 4$) had significant smaller coronary artery size than that of not-improved coronary vessels [2.0 ± 0.4 ($n = 4$) vs. 3.9 ± 0.4 ($n = 10$) mm, $p < 0.001$].

Fusion images

Representative case 1

A 48-year-old male with suspected CAD had cardiac CT and myocardial SPECT for the purpose of coronary artery

evaluation (Fig. 3). Myocardial scintigraphy by QPS showed the hypoperfusion in anteroseptum and apex of the left ventricle and the fill-in of the tracer in these lesions. Curved MPR image of LAD artery on CTA shows a calcification and stenosis of proximal LAD. The coronary angiogram revealed a 75% stenosis in the proximal segment of LAD.

Representative case 2

A 77-year-old male had myocardial infarction. Fusion SPECT/CTA image revealed total occlusion of first diagonal branch. Anterolateral perfusion defect was caused by the culprit lesion which was clearly depicted by fusion image (Fig. 4).

Representative case 3

A 72-year-old female had hypoperfusion in the stress image and the fill-in of the tracer in the rest image. The myocardial ischemia in basal inferior segment was induced by the stenosis in the mid-RCA. The culprit lesion was accurately diagnosed by the fusion image (Fig. 5).

Discussion

Our study showed that it is possible to make fusion image using cardiac CTA and MPI among different manufacturing company. And the fusion image of SPECT/CTA added diagnostic information on pathophysiologic lesion severity which was not obtained by side-by-side analysis.

The evaluation for known or suspected CAD using ECG-gated SPECT imaging has been established for its diagnosis and risk assessment [18–20]. It is a well-known fact that a comprehensive assessment of CAD requires not only morphologic information about coronary stenosis location and degree but also functional information [21, 22]. And an imaging strategy, such as utilizing SPECT, is valuable to discern the extent and severity of provocative ischemia, and the location of the ischemia [23]. Because MPI does not contain coronary artery information, the fusion image between SPECT and CTA has a potential to make nuclear cardiology more useful in clinical medicine [10, 24, 25].

Recent introduction of CTA has greatly benefited cardiovascular imaging application [4]. The CTA has emerged as an alternative to invasive coronary angiography with good diagnostic accuracy in selected patients [4, 5]. Observation from 64-slice CTA provides high-quality noninvasive coronary arteriogram that accurately delineates the presence or absence of significant stenotic lesion within entire coronary trees [4, 5]. However, recent reports

Fig. 3 Fusion image between cardiac CTA and SPECT in 48-year-old male patient. CTA shows coronary vessels and cardiac SPECT shows hypoperfusion in anteroseptum and apex of the left ventricle in the stress and rest images. Culprit lesion is indicated by yellow arrow. **a** Curved multiplanar reconstruction image of LAD artery shows a calcification and stenosis of proximal LAD. **b** The coronary angiogram reveals a 75% stenosis in the proximal segment of a LAD

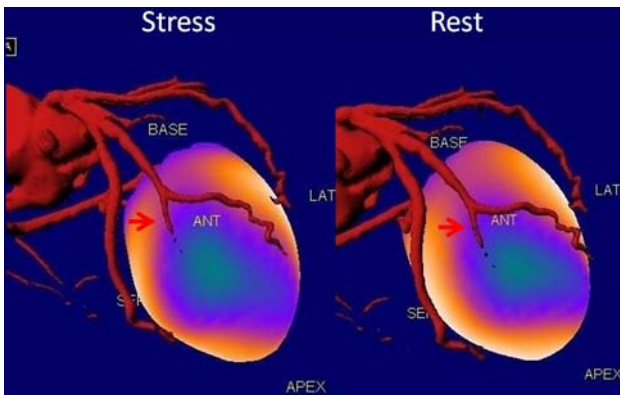
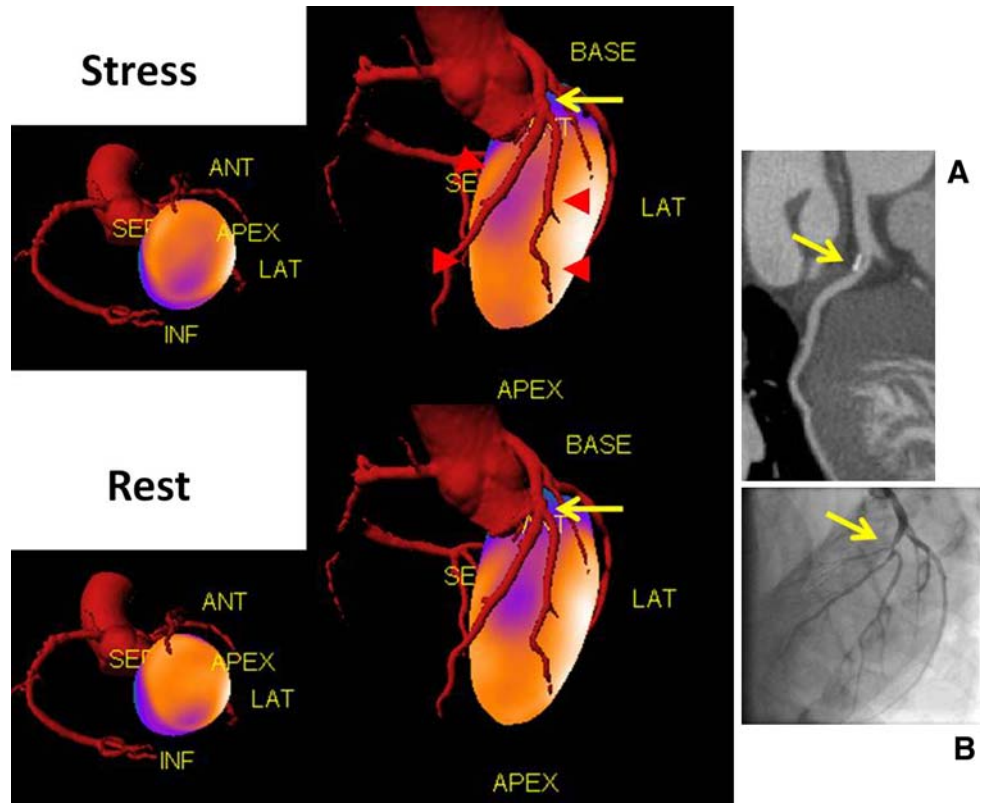


Fig. 4 A 77-year-old male had myocardial infarction. Fusion SPECT/CTA image revealed total occlusion of first diagonal branch. Anterolateral perfusion defect was caused by the lesion as shown by red arrow. LAD left anterior descending coronary artery, LCX left circumflex coronary artery, D1 first diagonal branch

showed that CTA does not predict the functional relevance of coronary artery stenoses in patients with stable angina in accordance with our result [7, 22]. The potential clinical value of such information remains to be elucidated. Therefore, the policy of proceeding directly with CTA stenosis for the intervention results in subjecting patients to a higher number of cardiac events, because CTA stenosis is irrelevant with functional ischemia, as shown in this study [3, 7, 22].

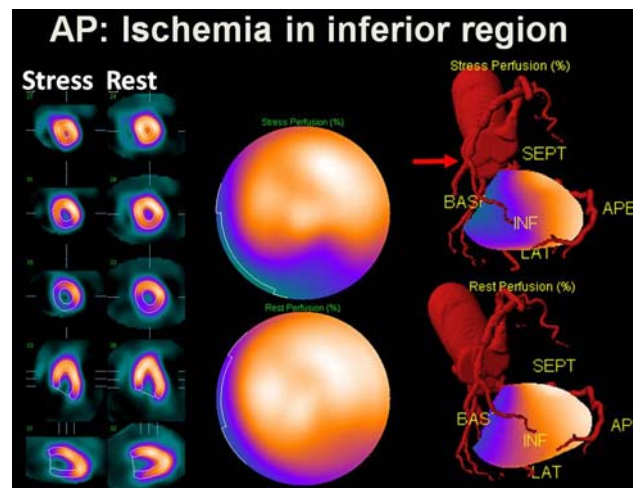


Fig. 5 A 72-year-old female had hypoperfusion in the stress image and the fill-in of the tracer in the rest image. The myocardial ischemia in basal inferior segment was induced by the stenosis in the mid-right coronary artery (red arrow)

Software-based cardiac fusion image between SPECT and CTA may offer better diagnostic information with regard to identification of culprit lesion and increase diagnostic confidence for categorizing intermediate lesions and equivocal perfusion abnormalities [10, 26, 27]. Previous studies showed that fusion images of coronary vessels

and myocardial perfusion facilitate assessment of the hemodynamic significance of coronary stenosis [6]. Although the creation of a fusion image has various kinds of procedures, there is a clinical report about diagnosis by a single maker using commercially available software [6]. Its measurement was rather challenging and the chosen method is recognized as an approximation because 3D surfaces of QPS are not the same as the surface of the heart. The creation of the SPECT/CTA fusion imaging in different manufacturers may make it possible to enhance the use of fusion image and the techniques. The great value of hybrid imaging among different manufactures was confirmed in this study in accordance with previous studies [6]. This study demonstrated that fusion SPECT/CTA offers such diagnostic confidence provided by myocardial perfusion defect distal to a vessel stenosis detected on CTA in accordance with previous studies [6, 24]. Furthermore, a high confidence in image interpretation as the occurrence of equivocal findings in one modality may be supplemented by the other. We have included patients with bypass-graft operation in which culprit lesion is difficult to determine. More number of doctors, including cardiologists and internist, should easily understand the relationship between the diseased coronary artery and myocardial perfusion.

The present results may have important clinical implications. The use of fusion image may increase the information obtained from each separate scan at no additional cost. And precise therapy to the culprit lesion may become possible, if provided with integrated evaluation of anatomy and physiology in a noninvasive way. Coronary interventionalists may be able to make decision for the target vessels. And after successful coronary intervention of the infarct-related vessel, a fusion imaging may be used to assess the ischemic potential of obstructive CAD remote from infarcted zone. Further studies are needed to investigate gated SPECT, calcium scores and CTA to make diagnostic algorithm in known or suspected CAD.

QPS image does not have the location information. Actually, CT coronary trees may not be the most suitable for determining the left ventricular positions. The further technical improvements are needed in precise registration of the images.

Conclusion

Quantitative perfusion SPECT-based cardiac SPECT/CTA fusion imaging provides additional information about hemodynamic relevance and exact allocation of perfusion abnormalities to its subtending coronary artery.

Acknowledgments We thank Mr. Masato Yamada and staffs of division of cardiovascular medicine and department of radiology at Kanazawa University Hospital for technical assistance.

References

1. Nishimura T, Nakajima K, Kusuoka H, Yamashina A, Nishimura S. Prognostic study of risk stratification among Japanese patients with ischemic heart disease using gated myocardial perfusion SPECT: J-ACCESS study. *Eur J Nucl Med Mol Imaging*. 2008;35:319–28.
2. Tamaki N. Guidelines for clinical use of cardiac nuclear medicine (JCS 2005). *Circ J*. 2005;69(Suppl IV):1125–202.
3. Matsuo S, Nakajima K, Horie M, Nakae I, Nishimura T. Prognostic value of normal stress myocardial perfusion imaging in Japanese population: a study based on the J-ACCESS study. *Circ J*. 2008;72:611–7.
4. Miller JM, Rochitte CE, Dewey M, Arbab-Zadeh A, Niinuma H, Gottlieb I, et al. Diagnostic performance of coronary angiography by 64-row CT. *N Engl J Med*. 2008;359:2324–36.
5. Matsuo S, Nakamura Y, Matsumoto T, Nakae I, Nagatani H, Takazakura R, et al. Visual assessment of coronary artery stenosis with electrocardiographically-gated multislice computed tomography. *Int J Cardiovasc Imaging*. 2004;20:61–6.
6. Gaemperli O, Schepis T, Valenta I, Husmann L, Scheffel H, Duerst V, et al. Cardiac image fusion from stand-alone SPECT and CT: clinical experience. *J Nucl Med*. 2007;48:696–703.
7. Hacker M, Jakobs T, Hack N, Nikolaou K, Becker C, von Ziegler F, et al. Sixty-four slice spiral CT angiography does not predict the functional relevance of coronary artery stenoses in patients with stable angina. *Eur J Nucl Med Mol Imaging*. 2007;34:4–10.
8. Hacker M, Jakobs T, Matthiesen F, Nikolaou K, Becker C, Knez A, et al. Combined functional and morphological imaging consisting of gated myocardial perfusion SPECT and 16-detector multislice spiral CT angiography in the noninvasive evaluation of coronary artery disease: first experiences. *Clin Imaging*. 2007;31:313–20.
9. Nakajo H, Kumita S, Cho K, Kumazaki T. Three-dimensional registration of myocardial perfusion SPECT and CT coronary angiography. *Ann Nucl Med*. 2005;19:207–15.
10. Schindler TH, Magosaki N, Jeserich M, Oser U, Krause T, Fischer R, et al. Fusion imaging: combined visualization of 3D reconstructed coronary artery tree and 3D myocardial scintigraphic image in coronary artery disease. *Int J Card Imaging*. 1999;15:357–68.
11. Germano G, Kavanagh PB, Slomka PJ, Van Kriekinge SD, Pollard G, Berman DS. Quantitation in gated perfusion SPECT imaging: the Cedars-Sinai approach. *J Nucl Cardiol*. 2007;14:433–54.
12. Nishimura Y, Fukuchi K, Katafuchi T, Sagou M, Oka H, Ishida Y, et al. Superimposed display of coronary artery on gated myocardial perfusion scintigraphy. *J Nucl Med*. 2004;45:1444–9.
13. Sato Y, Matsumoto N, Kato M, Inoue F, Horie T, Kusama J, et al. Noninvasive assessment of coronary artery disease by multislice spiral computed tomography using a new retrospectively ECG-gated image reconstruction technique. *Circ J*. 2003;67:401–5.
14. Austen WG, Edwards JE, Frye RL, Gensini GG, Gott VL, Griffith LS, et al. A reporting system on patients evaluated for coronary artery disease. Report of the Ad Hoc Committee for Grading of Coronary Artery Disease, Council on Cardiovascular Surgery, American Heart Association. *Circulation*. 1975;51(4 Suppl):5–40.
15. Matsumoto N, Sato Y, Suzuki Y, Kunimasa T, Yoda S, Iida J, et al. Prognostic value of myocardial perfusion single-photon emission computed tomography for the prediction of future

- cardiac events in a Japanese population: a middle-term follow-up study. *Circ J*. 2007;71:1580–5.
16. Cerqueira MD, Weissman NJ, Dilsizian V, Jacobs AK, Kaul S, Laskey WK, et al. American Heart Association Writing Group on myocardial segmentation and registration for cardiac imaging standardized myocardial segmentation and nomenclature for tomographic imaging of the heart: a statement for healthcare professionals from the Cardiac Imaging Committee of the Council on Clinical Cardiology of the American Heart Association. *Circulation*. 2002;105:539–42.
 17. Malkemecker D, Brenner R, Martin WH, Sampson UK, Feurer ID, Kronenberg MW, et al. CT-based attenuation correction versus prone imaging to decrease equivocal interpretations of rest/stress Tc-99 m tetrofosmin SPECT MPI. *J Nucl Cardiol*. 2007;14:314–23.
 18. Matsuo S, Matsumoto T, Nakae I, Koh T, Masuda D, Takada M, et al. Prognostic value of ECG-gated thallium-201 single-photon emission tomography in patients with coronary artery disease. *Ann Nucl Med*. 2004;18:617–22.
 19. Matsuo S, Nakae I, Matsumoto T, Horie M. Impact of endothelial dysfunction on left ventricular remodeling after successful primary coronary angioplasty for acute myocardial infarction—analysis by quantitative ECG-gated SPECT. *Ann Nucl Med*. 2006;20:57–62.
 20. Matsuo S, Nakamura Y, Tsutamoto T, Kinoshita M. Impairments of myocardial sympathetic activity may reflect the progression of myocardial damage or dysfunction in hypertrophic cardiomyopathy. *J Nucl Cardiol*. 2002;9:407–12.
 21. Gaemperli O, Schepis T, Koepfli P, Valenta I, Soyka J, Leschka S, et al. Accuracy of 64-slice CT angiography for the detection of functionally relevant coronary stenoses as assessed with myocardial perfusion SPECT. *Eur J Nucl Med Mol Imaging*. 2007;34:1162–71.
 22. Meijboom WB, Van Mieghem CA, van Pelt N, Weustink A, Pugliese F, Mollet NR, et al. Comprehensive assessment of coronary artery stenoses: computed tomography coronary angiography versus conventional coronary angiography and correlation with fractional flow reserve in patients with stable angina. *J Am Coll Cardiol*. 2008;52:636–43.
 23. Tanihata S, Nishigaki K, Kawasaki M, Takemura G, Minatoguchi S, Fujiwara H. Outcomes of patients with stable low-risk coronary artery disease receiving medical- and PCI-preceding therapies in Japan: J-SAP study 1–1. *Circ J*. 2006;70:365–9.
 24. Nakaura T, Utsunomiya D, Shiraishi S, Tomiguchi S, Honda T, Ogawa H, et al. Three-dimensional cardiac image fusion using new CT angiography and SPECT methods. *AJR*. 2005;185:1554–7.
 25. Tanaka A, Shimada K, Yoshida K, Jissyo S, Tanaka H, Sakamoto M, et al. Non-invasive assessment of plaque rupture by 64-slice multidetector computed tomography—comparison with intravascular ultrasound. *Circ J*. 2008;72:1276–81.
 26. Gaemperli O, Schepis T, Kalff V, Namdar M, Valenta I, Stefani L, et al. Validation of a new cardiac image fusion software for three-dimensional integration of myocardial perfusion SPECT and stand-alone 64-slice CT angiography. *Eur J Nucl Med Mol Imaging*. 2007;34:1097–106.
 27. Faber TL, Santana CA, Garcia EV, Candell-Riera J, Folks RD, Peifer JW, et al. Three-dimensional fusion of coronary arteries with myocardial perfusion distributions: clinical validation. *J Nucl Med*. 2004;45:745–53.